The University of
Nottingham

UNITED KINGDOM · CHINA · MALAYSIA

Torcello-Gómez, Amelia and Foster, Tim (2014) Interactions between cellulose ethers and a bile salt in the control of lipid digestion of lipid-based systems. Carbohydrate Polymers, 113 . pp. 53-61. ISSN 1879-1344

Access from the University of Nottingham repository:

http://eprints.nottingham.ac.uk/45454/8/Manuscript_Torcello%20et%20al_just%20accepted%20manuscript.pdf

1 INTERACTIONS BETWEEN CELLULOSE ETHERS AND A BILE SALT IN THE

2 CONTROL OF LIPID DIGESTION OF LIPID-BASED SYSTEMS

3

4 Amelia Torcello-Gómez[a],* and Timothy J. Foster[a]

5

6 [a]Division of Food Sciences, School of Biosciences, University of Nottingham, Sutton

7 Bonington Campus, Loughborough, LE12 5RD, United Kingdom, email addresses:

8 amelia.torcello_gomez@nottingham.ac.uk, tim.foster@nottingham.ac.uk

9

10 Corresponding author (*): Division of Food Sciences, School of Biosciences, University of
11 Nottingham, Sutton Bonington Campus, Loughborough, LE12 5RD, United Kingdom

12 Email address: amelia.torcello_gomez@nottingham.ac.uk (A. Torcello-Gómez)

13 Tel: +44 (0)115 951 6197

14 Fax: +44 (0)115 951 6142

15

16

17

18

19

20

21

22

23

24

25

26

ABSTRACT

In order to gain new insights into the potential of specific dietary fibres to control lipid digestion, the goal of this work is to study the main interactions between commercial cellulose ethers, as dietary fibre, and a bile salt, as an important duodenal component present during the digestibility of lipids. These interactions have been evaluated in two different scenarios found for an oil-in-water emulsion on its transit through the duodenum. Namely, interactions in the continuous phase and competitive adsorption at the oil–water interface have been looked at by means of micro-differential scanning calorimetry (micro-DSC) and interfacial tension (IT). Micro-DSC revealed that the presence of the bile salt affects the thermogelation process of cellulose derivatives, suggesting binding to cellulose ethers. The effect on thermogelation seems to be cellulose type-dependent. IT measurements proved the ability of cellulose ethers to compete for the oil–water interface in the presence of the bile salt. Interactions in the bulk might have an impact on this interfacial scenario. These findings may have implications in the digestion of emulsified lipids, hence providing a springboard to develop new cellulose-based food products with improved functional properties.

Keywords: dietary fibre, cellulose ethers, bile salts, oil–water interface, interfacial tension, differential scanning calorimetry.

1. INTRODUCTION

Cellulose derivatives belong to a wide group called dietary fibres which have been shown to provide health benefits in the diet by, for instance, lowering blood cholesterol (Anderson & Siesel, 1990; Kritchevsky & Story, 1993). This is due to the ability of certain types of dietary fibre to interfere with the process of digestion in a number of different and related ways. On the one hand, dietary fibres bind bile salts in the duodenum which are sequestered and eventually excreted (Story, Furumoto, & Buhman, 1997). Hence, dietary fibres reduce bile re-absorption, inducing the synthesis of bile salts from blood cholesterol to restore the content lost (Lee, Kim, & Kim, 1999; Zarras & Vogl, 1999). On the other hand, an alternative mechanism proposed to explain the reduction of blood cholesterol levels by dietary fibre is the prevention of lipid absorption (Jenkins, Kendall, & Ransom, 1998; Lairon, 1996; Yokoyama et al., 2011), which can be partially related to the sequestration of bile salt due to binding. Indeed, the binding mechanism may influence lipid absorption by affecting the process of lipid digestion. This is because bile salts play a crucial role in lipid digestion within the duodenum (upper small intestine), where the majority of this process occurs, *c.a.* 70-90% (Fave, Coste, & Armand, 2004). When lipids eventually reach the small intestine, they are normally present as small lipid droplets dispersed in a compositionally and structurally complex aqueous medium. Bile salts are secreted into the duodenum and adsorb onto the surface of lipid droplets to further emulsify them and to prepare this interface for the enzymatic breakdown by the pancreatic lipase. This enzyme anchors to the lipid-water interface with the help of its cofactor colipase, previously adsorbed on the bile salt-covered interface, by forming a lipase-colipase complex (Reis, Holmberg, Watzke, Leser, & Miller, 2009). Lipase then hydrolyses the lipids (lipolysis), mainly composed of triglycerides, into free fatty acids, monoglycerides and diglycerides. Some of these products are soluble, so that

76 they can be removed from the surface of lipid droplets and become incorporated within

77 micelles/vesicles of bile salts in order to be absorbed by the intestinal mucosa.

78 Therefore, any way whereby dietary fibre can interfere with the above process may also

79 affect the rate of lipid digestion and hence absorption. Several possible mechanisms that may

80 alter this process include the binding of dietary fibre to bile salts or to the enzymes, the

81 adsorption of dietary fibre on the oil–water interface, forming a protective layer against the

82 action of bile salts and lipase, and intraluminal disruption of mixed micelles of digested lipids

83 and bile salts, reducing transport into the mucosal surface barrier (Vahouny et al., 1988).

84 Despite the known ability of dietary fibres to influence lipid absorption, to our best

85 knowledge there is a need of fundamental studies on their potential to control lipid digestion

86 (Beysseriat, Decker, & McClements, 2006; Tokle, Lesmes, Decker, & McClements, 2012).

87 Previous work in literature reported on electrostatic interactions between chitosan and a bile

88 salt (Thongngam & McClements, 2005), dynamic molecular contact of beta-glucan with a

89 bile salt and entrapment of bile micelles by an arabinoxylan matrix without direct molecular

90 interaction (Gunness, Flanagan, & Gidley, 2010). However, the mechanisms by which dietary

91 fibres interact with bile salts in the digestive tract are still not known. Hence, a systematic

92 approach should be taken to identify the dominant mechanism for each specific type of

93 dietary fibre to influence lipid digestion, in order to better understand the underlying

94 molecular effects of digestion conditions in real complex food emulsions containing specific

95 dietary fibres.

96 A previous study on the interactions between synthetic polymeric surfactants and bile salts in

97 oil-in-water emulsions has shown that binding of these polymers to a bile salt may have an

98 impact on the interfacial properties of the emulsions related to access for digestion (Torcello-

99 Gómez, Maldonado-Valderrama, Jódar-Reyes, & Foster, 2013). Cellulose derivatives offer a

100 good candidate mirroring the block-copolymer research. For that reason, the aim of this work

101   is to study the main interactions between cellulose derivatives, as non-ionic dietary fibre, and

102   bile salts, as an important duodenal component. Specifically, we have focused on the

103   interactions in the aqueous phase and competitive adsorption at the oil–water interface as

104   scenarios of oil-in-water emulsions as they pass through the duodenum. These interactions

105   have been characterised in the aqueous phase by means of micro-differential scanning

106   calorimetry, and at the oil–water interface through competitive adsorption by means of

107   interfacial tension measurements. This combination of techniques has shown to be successful

108   in previous work (Torcello-Gómez et al., 2013).

109   Commercial cellulose ethers have been chosen as dietary fibre due to the highly functional

110   properties which are important in the manufacture process of food, such as: surface activity,

111   binding, thickening, and a wide range of viscosities. For the cellulose derivatives chosen, the

112   native cellulose backbone has been chemically modified by partially reacting the hydroxyl

113   groups in each sugar ring (Table 1) to provide the following cellulose ethers: methylcellulose

114   (MC), in which methyl group is the sole substituent, hydroxypropylmethylcellulose (HPMC)

115   in which methyl group remains the dominant substituent, but incorporating smaller amounts

116   of the larger and more polar hydroxypropyl group, and hydroxypropylcellulose (HPC) where

117   the hydroxypropyl group is the sole substituent. These are three of the four cellulose

118   derivative forms used in the food area for their surface tension reducing properties (Mezdour,

119   Cuvelier, Cash, & Michon, 2007). This selection allows us to discuss the results comparing

120   their molecular properties, such as the molecular weight in the case of MC, and the type and

121   number of substituents for a set of cellulose ethers within the same range of viscosity (MC,

122   HPMC and HPC) and hence molecular weight (see Table 1), since the viscosity of aqueous

123   solutions of cellulose ethers is proportional to its molecular weight. Sodium

124   taurodeoxycholate (NaTDC) was used as an example of a typical bile salt, since bile salts
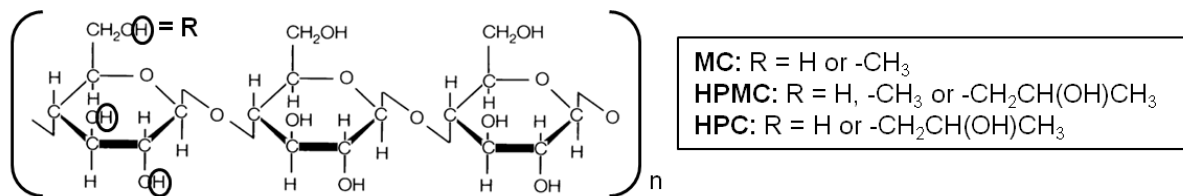
125 behave in a qualitative similar manner despite their large variety (Maldonado-Valderrama,

126 Wilde, Macierzanka, & Mackie, 2011).

127 Beginning to quantify the dynamics of interactions in the bulk and the impact that has on the

128 interfacial properties, related to access for digestion, provides new insights for designing

129 rules for application. These new findings can be exploited in tailoring both novel food and

130 pharmacological matrices with improved functional properties.

131

132 **Table 1.** Physicochemical characteristics of the cellulose ethers (Sarkar, 1979).

Cellulose Ether		$DS_{methoxyl}$	$MS_{hydroxypropyl}$	Viscosity range (mPa·s)	MW range (KDa)
MC	A4C	1.8	0	400 (2 wt%)	120-150
	A4M			4000 (2 wt%)	300-500
HPMC	K4M	1.4	0.21	4000 (2 wt%)	300-500
HPC	HF	0	4	1500-3000 (1 wt%)	1115

MC: R = H or -CH₃
HPMC: R = H, -CH₃ or -CH₂CH(OH)CH₃
HPC: R = H or -CH₂CH(OH)CH₃

133

134

135 2. MATERIALS AND METHODS

136 *2.1. Materials*

137 METHOCEL™ A4C, A4M and K4M from the Dow Chemical Company were used without

138 purification. The initial letter 'A' denotes MC and 'K' corresponds to HPMC. In each case,

139 '4C' and '4M' denote a solution viscosity of 400 and 4000 mPa·s, respectively, measured at

140   2 wt% concentration under standard conditions in a capillary viscometer. Klucel® HPC HF

141   was purchased from Hercules. The different levels of incorporation of the two substituents

142   (degree of substitution, DS, and molar substitution, MS) and range of viscosities are indicated

143   in Table 1.

144   The bile salt used in this study is sodium taurodeoxycholate (NaTDC, 97% purity) from

145   Sigma-Aldrich. It is negatively charged at pH 7 and its molecular weight is 521.7 g/mol.

146   The aqueous phase was 1.13 mM phosphate buffer (pH 7) prepared with ultrapure water

147   purified in a Pur1te Select system.

148   Highly refined olive oil was also purchased from Sigma-Aldrich, and purified with activated

149   magnesium silicate (Florisil®, Fluka) to eliminate free fatty acids and surface active

150   impurities. Namely, a mixture of oil and Florisil® in proportion 2:1 wt/wt was shaken mildly

151   for 3 h and centrifuged at 4000 rpm for 30 min in a bench centrifuge. It was then filtered

152   through Whatman filter paper #1 under vacuum and stored away from light.

153

154   *2.2. Sample Preparation*

155   Cellulose ethers stock solutions (2 wt%) were prepared as follows. Approximately one-third

156   of the required final volume of aqueous phase was heated to ~80 °C, and then cellulose ether

157   powder was added carefully under stirring. The complete solubilisation was obtained by

158   adding the remaining aqueous phase at room temperature and continuing the agitation of the

159   solution for at least 2 h at room temperature. It was then stored at 4 °C overnight to achieve

160   the maximum hydration, and without stirring to eliminate air bubbles. Aliquots from the

161   stock solutions were dried at 50 °C overnight to confirm that the final concentration was 2

162   wt%. Different concentrations were obtained by successive dilution from the concentrated

163   stock.

164 NaTDC stock solution was prepared by dissolving the powder in the aqueous phase at room

165 temperature under stirring for at least 1 h. Then, the stock solution was successively diluted

166 to obtain different concentrations.

167 Mixed cellulose ethers-NaTDC solutions were prepared from aliquots of cellulose ethers and

168 NaTDC solutions at room temperature, in various proportions. The final concentration of

169 cellulose ethers was fixed at 0.3 and 1 wt% for micro-DSC experiments and at 10^{-3} wt% for

170 interfacial tension measurements, whereas the final concentration of NaTDC ranged from 0

171 to 100 mM.

172

173 *2.3. Micro-Differential Scanning Calorimetry (micro-DSC)*

174 The bulk properties of cellulose ethers in the absence and presence of bile salt were studied

175 by characterising the thermal events of the samples in a Micro-Differential Scanning

176 Calorimeter (DSC III Setaram, Caluire, France). About 800 mg of each sample were sealed

177 into the DSC cells made from Hastalloy. The reference cell was filled with the same weight

178 of phosphate buffer and coordinated for heat capacity with the sample. Sample and reference

179 cells were initially cooled to a starting temperature of 5 °C to equilibrate. Cells were then run

180 at a scanning rate of 1 °C/min from 5 to 110 °C, cooled and rerun while all steps were

181 recorded. The heating rate was selected as a compromise between the need for proximity to

182 the equilibrium (heating rate as low as possible) and an acceptable signal/disturbance ratio

183 (heating rate not too low). Enthalpy values were calculated using Setaram software with a

184 linear interpolated baseline, based on an extension of the trace before and after the thermal

185 event.

186

187 *2.4. Interfacial Tension and Dilatational Rheology*

188 Adsorption of cellulose ethers at the olive oil–water interface, alone or in competitive

189 adsorption with the bile salt, was characterised by means of a Profile Analysis Tensiometer

190 (PAT1, SINTERFACE Technologies, Germany). For this purpose, the interfacial tension was

191 recorded at constant interfacial area during 30 min. The apparatus is computer-controlled; the

192 software fits the experimental drop profile to the Young-Laplace equation of capillarity

193 providing as output the drop volume V, the interfacial tension γ, and the interfacial area A.

194 The aqueous droplet was formed at the tip of the capillary and immersed in a glass cuvette,

195 which contained the oil phase, placed in a thermostatically controlled cell at 20 ºC. The

196 interfacial tension of the clean interface (oil–water) was measured before every experiment to

197 ensure the absence of surface-active contaminants obtaining values of (29.5 ± 0.5) mN/m at

198 20 ºC. The materials in contact with the solutions were properly cleaned in order to avoid any

199 contamination by any surface active substance.

200 Measurements of the interfacial dilatational rheology were made at the end of the adsorption

201 period by inducing sinusoidal oscillations to the interface, by injecting and extracting volume

202 into and from the droplet, while the response in the interfacial tension was recorded. The

203 dilatational parameters of the interfacial layers were calculated via a Fourier transformation

204 algorithm implemented in the software analysis. In a general case, the dilatational modulus

205 (E) is a complex quantity that contains a real and an imaginary part:

$$E = E' + iE'' = \varepsilon + i2\pi f\eta \tag{1}$$

207 where E' is the storage modulus or the elasticity (ε) of the interfacial layer and E'' is the loss

208 modulus that accounts for the viscosity (η) of the interfacial layer. The applied interfacial

209 area oscillations were maintained at 5 % of amplitude to avoid excessive perturbation of the

210 interfacial layer and the departure from the linear viscoelastic region (Camino, Perez,

211 Sanchez, Patino, & Pilosof, 2009; Mezdour, Lepine, Erazo-Majewicz, Ducept, & Michon,

212 2008). The oscillation frequency (f) ranged from 0.01 to 0.3 Hz.

213   The reproducibility of the experiments was verified from the standard deviation of at least

214   three replicate measurements.

215

216   3. RESULTS AND DISCUSSION

217   Interactions between cellulose ethers and the bile salt will be studied separately in the

218   aqueous phase and at the oil–water interface to account for different scenarios of an oil-in-

219   water emulsion in the duodenum stage of digestion; that is the bulk phase and surface of oil

220   droplets in the presence of bile salts. In addition, in both areas of study, corresponding to

221   aqueous phase or oil–water interface, the behaviour of cellulose ethers alone will be

222   considered, as a reference, before comparing with the behaviour of mixtures of cellulose

223   ethers and bile salt.

224

225   *3.1. Bulk properties of cellulose ethers*

226   Firstly, the effect of the molecular weight on the bulk properties of cellulose alone is

227   considered by comparing the micro-DSC traces for two samples with the same type and

228   number of substituents but different range of viscosity and hence molecular weight. Namely,

229   MC A4C (lower molecular weight) and A4M (higher molecular weight) are compared in

230   Figure 1a. The thermograms of both types of MC display an endothermic peak on heating

231   which appears exothermic on cooling. This thermal transition corresponds to the gelation

232   process of MC, which has been previously characterised by a combination of techniques,

233   such as DSC and rheology, by Haque and co-workers (Haque & Morris, 1993). As observed

234   in Figure 1a, the temperature-course of thermogelation is comparable for both A4C and A4M

235   upon heating and cooling. Furthermore, the transition enthalpy values measured from the area

236   below the peaks on heating and on cooling for A4C and A4M, which are also shown in

237   Figure 1, are similar within the margin of error. These observations can be explained by the

238   presumably similar content of hydrophobic substituents, *i.e.* methyl groups, in both types of

239   MC and are therefore not molecular weight dependant.

240
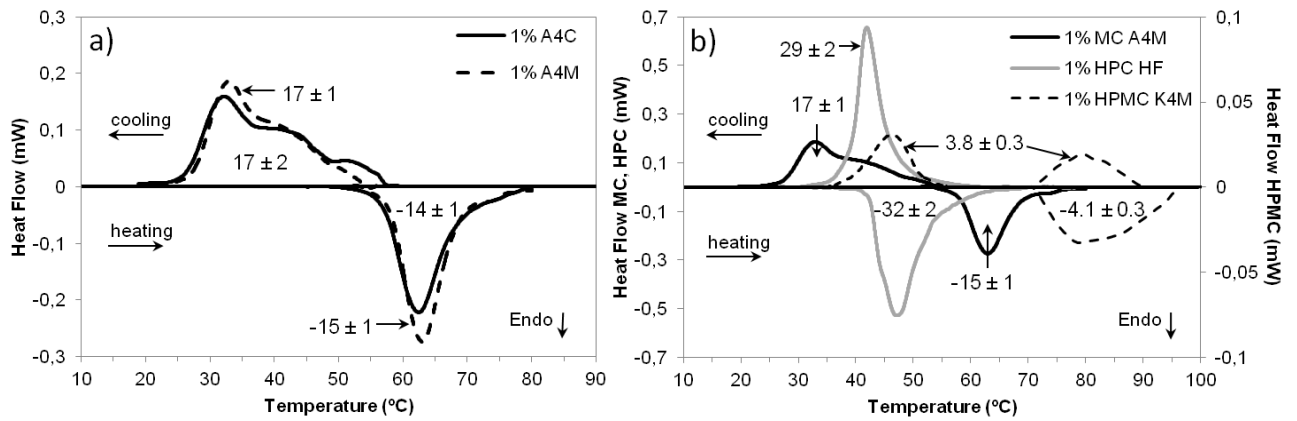
241

242   **Figure 1:** Micro-DSC traces on heating and on cooling of a) 1 wt% MC solutions: low

243   molecular weight, A4C; high molecular weight, A4M; b) 1 wt% cellulose ether solutions; left

244   axis: MC A4M; HPC HF; right axis: HPMC K4M. Transition enthalpy values on heating and

245   on cooling are given in $J/g_{polymer}$.

246

247   Secondly, the effect of number and type of substituents on the bulk properties is evaluated for

248   the set of cellulose ethers within a similar range of viscosity: MC A4M, HPMC K4M and

249   HPC HF. Corresponding micro-DSC traces and the values of the transition enthalpy are

250   presented in Figure 1b for A4M, K4M and HF at 1 wt%. MC and HPC will be first compared

251   since they present different substituents, methyl or hydroxypropyl groups, respectively. Then,

252   the effect of the presence of both kinds of substituents in HPMC will be discussed, comparing

253   with the behaviour of MC and HPC. It can be seen in Figure 1b appreciable differences

254   between the thermograms of HPC and MC. HPC shows the highest values of transition

255   enthalpy, "demixes" at lower temperature on heating and displays slight thermal hysteresis

256   when re-dissolving on cooling, as compared to MC. Previous studies proposed different

257   mechanisms of thermal transition for cellulose ethers (Haque & Morris, 1993; Haque,

258   Richardson, Morris, Gidley, & Caswell, 1993; Sun et al., 2009), which are summarised here

259   to explain the differences found for HPC and MC (Figure 2). In the case of HPC which is

260   highly substituted (Table 1), the more "uniform" distribution of hydroxypropyl groups along

261   the polymer chains would allow the hydrophobic association to take place in one step upon

262   heating. Differently, gelation of MC comprises at least two steps. MC is found in solution as

263   bundles where strands are held together by packing of unsubstituted regions and by

264   hydrophobic clustering of methyl groups in regions of denser substitution. In a first step upon

265   heating, the strands separate at the ends of the bundles and methyl groups are exposed. This

266   allows the second step to take place upon further increasing temperature, that is, the

267   association of hydrophobic regions of strands from different bundles (Figure 2).

268
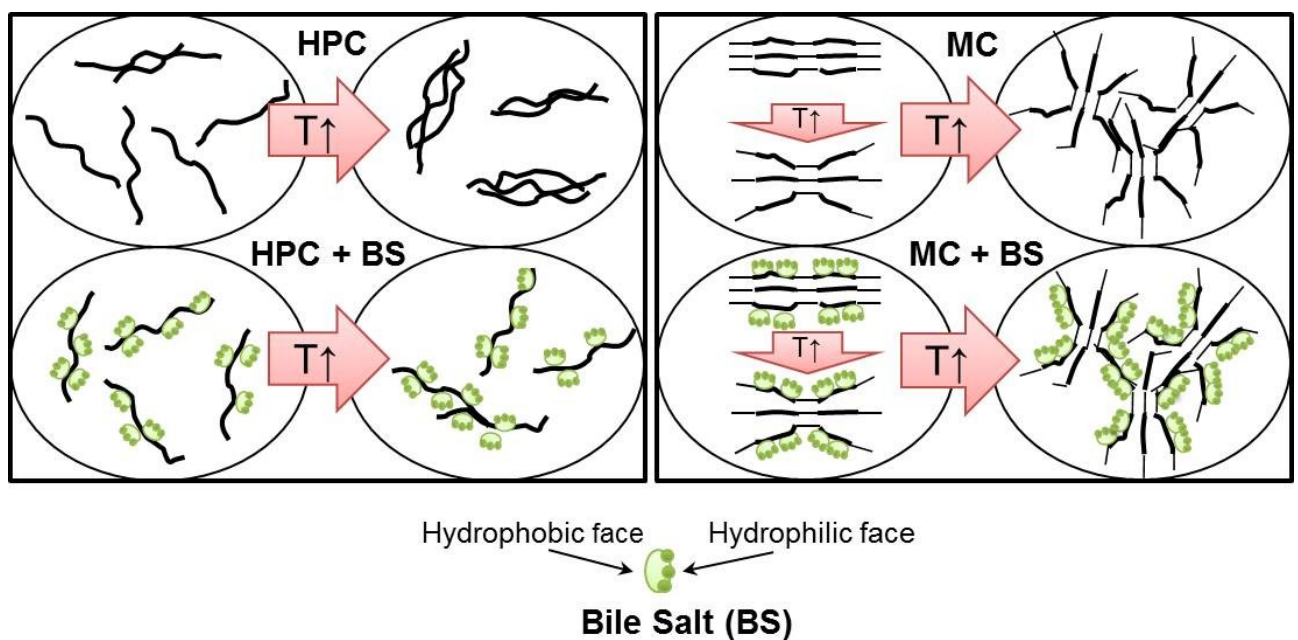
269

270   **Figure 2:** Schematic representation of the hypothetical structures and processes involved in

271   the thermal transition of cellulose ethers, HPC and MC, in the absence and presence of the

272   bile salt. Faint lines in cellulose ethers denote unsubstituted or sparingly substituted chain

273   segments; bold lines denote regions of dense substitution. See text for detailed description.

274

275　On the other hand, HPMC shows the lowest values of the transition enthalpy and also gels at

276　higher temperature on heating, as compared to MC (Figure 1b). The mechanism of

277　thermogelation is similar to that for MC, however, differences can be explained not only by

278　the lower content of hydrophobic substituents due to its lower DS for methyl groups, but also

279　by the presence of more polar hydroxypropyl groups that inhibit the hydrophobic gelation

280　(Haque et al., 1993). What Haque and co-workers did not show, that we now present in

281　Figure 1b, is a high temperature exotherm for HPMC upon cooling. We tentatively ascribe

282　this to possible distributions of the methyl and hydroxypropyl substituents on the cellulose

283　bundles, which we are currently investigating. Hence, clearly the type, number and

284　distribution of substituents affect the bulk properties of cellulose ethers (Sullo, Wang,

285　Koschella, Heinze, & Foster, 2013) that may also affect the interactions with the bile salt, as

286　it will be discussed below.

287　Finally, the effect of bulk concentration on the thermal transition of cellulose ethers is studied

288　for MC (A4M) and HPC (HF) at 0.3 and 1 wt% (Figure 3). Micro-DSC traces of HPMC

289　K4M at the relatively low concentration of 0.3 wt% were not reported here due to the low

290　values of the transition enthalpy. It can be observed in Figure 3 that the temperature-course of

291　the thermal event is independent of concentration for both types of cellulose ether, although

292　transition-onset temperatures are slightly displaced to higher values when decreasing the bulk

293　concentration, and transition enthalpy remains constant when normalised per gram of

294　polymer. This behaviour will be useful when interpreting the data for cellulose ethers in the

295　presence of bile salt.

296
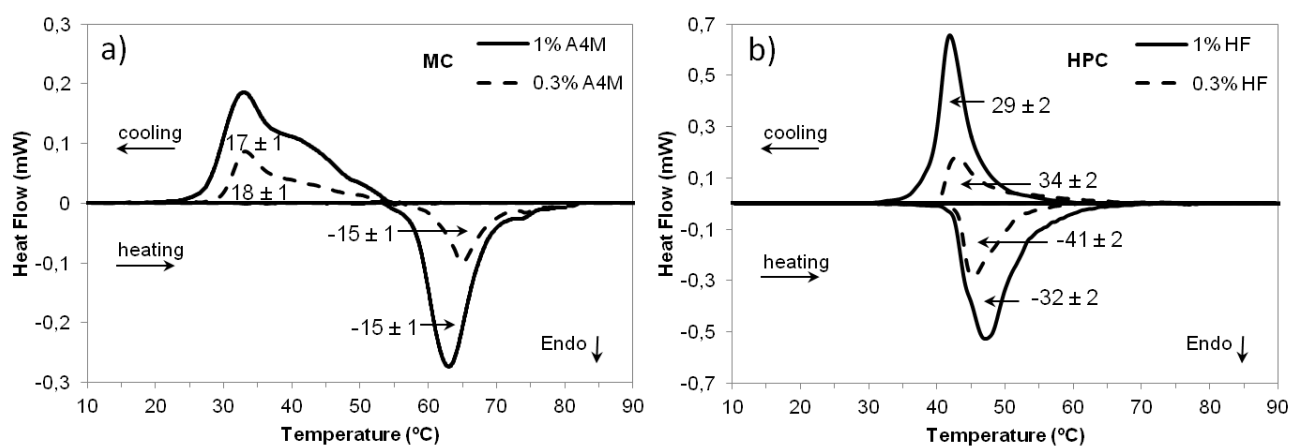
Figure 3: Micro-DSC traces on heating and on cooling of 0.3 and 1 wt% cellulose ether solutions: a) MC A4M; b) HPC HF. Transition enthalpy values on heating and on cooling are given in $J/g_{polymer}$.

3.2. Interactions between cellulose ethers and bile salt in the aqueous phase

In this section, similar micro-DSC experiments were carried out for mixtures of cellulose ethers at a fixed concentration of 0.3 and 1 wt% and the bile salt at concentrations varying from 0-100 mM in each case.

Figure 4 displays the peaks on heating and on cooling of cellulose ethers due to thermal transitions, in the absence and in the presence of the bile salt. Cellulose ethers within the same range of viscosity but with different number and type of substituents (MC A4M, HPMC K4M and HPC HF) were chosen for these experiments, since the thermal transition appears to be independent of the molecular weight for MC A4C and A4M. The most remarkable result is that the peak size gradually decreases upon increasing the bile salt concentration and even shift to higher temperatures, as observed in Figure 4. The shift is greater in the case of HPC, as compared to MC. This trend is also observed when the concentration of cellulose ethers was fixed at 0.3 wt% (data not shown). In the case of HPMC, the intermediate and highest concentrations of NaTDC shift the peaks to even a larger extent than for HPC. It

316 seems that the bile salt interacts with cellulose ethers affecting or even inhibiting the thermal

317 transition, as seen for HPMC at a bile salt concentration of 100 mM (Figure 4b).

318
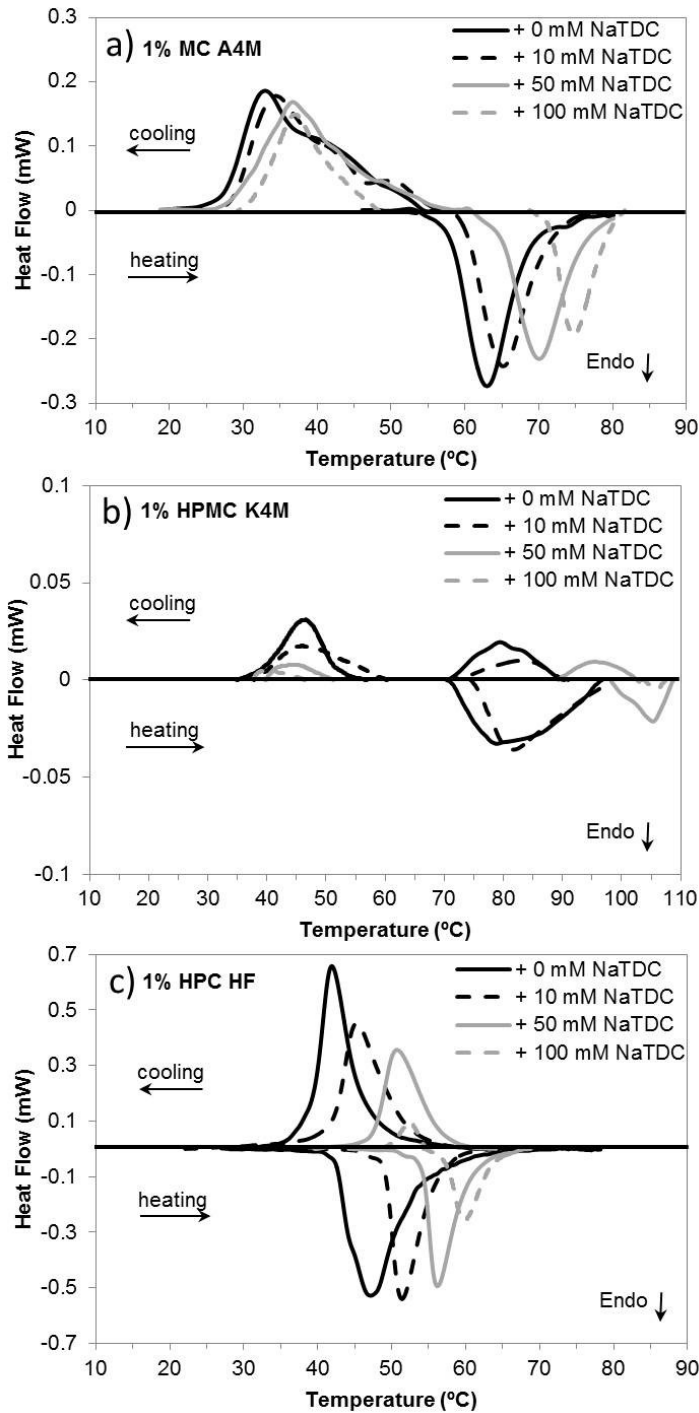
319

320 **Figure 4:** Micro-DSC traces on heating and on cooling of mixtures of 1 wt% cellulose ether

321 solutions and bile salt at several concentrations: a) MC A4M; b) HPMC K4M; c) HPC HF.

322

323   In order to analyse the effect of the type and number of substituents on these interactions with

324   the bile salt, the decrease in the transition enthalpy of cellulose ethers on heating is plotted as

325   a function of the bile salt concentration in Figure 5a. As a general trend, increasing the

326   concentration of bile salt decreases the transition enthalpy of cellulose ethers. However, there

327   are clear differences regarding the type and number of substituents. On the one hand, bile salt

328   reduces the transition enthalpy to a larger extent for HPMC and HPC within the whole range

329   of bile salt concentration, as compared to MC. As in the previous section, the effect of the

330   bile salt on thermal transition of cellulose ethers will be first compared for MC and HPC, and

331   then for HPMC.

332
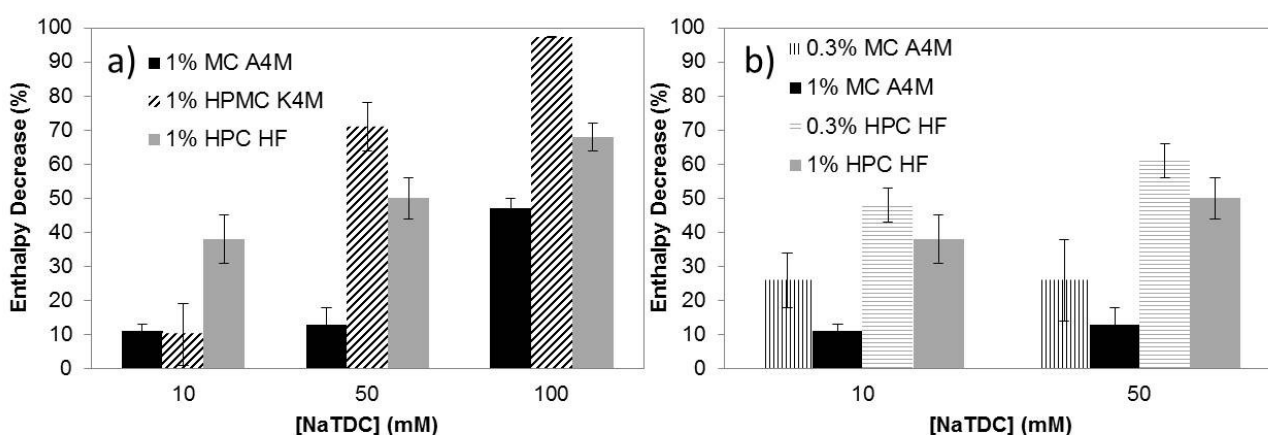
333
334   **Figure 5:** Decrease in transition enthalpy of cellulose ethers caused by the presence of the

335   bile salt: a) effect of the type and number of substituents; b) effect of bulk concentration.

336

337   We propose the following mechanism of interaction between cellulose derivatives and the

338   bile salt, which is illustrated in Figure 2, to explain the results, taking into account the model

339   proposed by Haque and co-workers (Haque & Morris, 1993; Haque et al., 1993). The

340   hydrophobic face of bile salt molecules adsorbs on the hydrophobic portions of cellulose

341   ethers, while the hydrophilic face exposures to the aqueous phase. In the case of HPC, the

342   more "uniform" distribution of bile salt along the polymer chains through the hydroxypropyl

343 groups would hinder the hydrophobic association upon heating. Differently for MC, bile salt

344 would adsorb to the methyl groups in the regions of denser substitution. Upon heating, the

345 recently exposed methyl groups would be still available, when the strands separate at the end

346 of the bundles, for the hydrophobic association of strands from different bundles to take place

347 (Figure 2). This then explains why the bile salt inhibits the thermal transition to a larger

348 extent for HPC as compared to MC regardless of the bile salt concentration, as well as the

349 larger shift of the peaks to higher temperature (Figures 4a,c; 5a). Next, the effect of the bulk

350 concentration of cellulose ethers on these interactions with the bile salt will be evaluated. For

351 this purpose, the decrease in the transition enthalpy of MC A4M and HPC HF is plotted for

352 the two concentrations studied, 0.3 and 1 wt%, as a function of the bile salt concentration in

353 Figure 5b. At a bulk concentration of 0.3 wt% for MC and HPC, again the bile salt decreases

354 to a greater extent the transition enthalpy for HPC, at all bile salt concentrations, as compared

355 to MC. This supports our hypothesis of interaction illustrated in Figure 2. However, the

356 enthalpy reduction by the bile salt is larger for MC and HPC at 0.3 wt% than at 1 wt%

357 (Figure 5b). This can be explained by the increase of the ratio bile salt/cellulose ether at this

358 lower bulk concentration of cellulose derivatives. The cellulose ether concentrations tested in

359 this study are well tolerated regarding future perspective of human health. On the other hand,

360 the bile salt concentrations used: 10, 50 and 100 mM, are above the physiological

361 concentration range in the fasted state in the human small intestine (3-7 mM). However, it

362 involves the physiological concentration range in the fed state (up to 20 mM). Since the

363 interactions between cellulose ethers and bile salt depend on the bile salt/cellulose ether ratio,

364 the cellulose ether concentration must be decreased to test higher bile salt/cellulose ether

365 ratios at physiological bile salt concentrations.

366 Finally, the mechanism of bile salt adsorption onto HPMC bundles would be similar to that

367 on MC (Figure 2). However, the lower content of methyl groups in HPMC and the presence

368 of the more polar hydroxypropyl groups would explain the results observed in Figure 5a.

369 Namely, the reduction in the transition enthalpy of HPMC by bile salt is much larger at

370 higher NaTDC concentrations, as compared to MC. The gel formed by HPMC is

371 substantially weaker than MC gel due to the presence of the larger hydroxypropyl

372 substituents that inhibit intermolecular association (Haque et al., 1993). To recall,

373 thermogelation of HPMC does not occur until higher temperature and the transition enthalpy

374 is considerably lower than for MC (Figure 1b). Interestingly, the resistance of hydroxypropyl

375 groups to incorporation in ordered structures upon heating seems to be magnified in the

376 presence of the bile salt, as observed at the highest bile salt concentration where the gelation

377 of HPMC is completely inhibited (Figures 4b; 5a).

378

379 *3.3. Interfacial activity of cellulose ethers at the oil–water interface*

380 Before considering the competitive adsorption of cellulose derivatives and bile salt at the oil–

381 water interface, first the interfacial activity of cellulose ethers alone is evaluated as a

382 reference. Few investigations have been focused on the behaviour of these cellulose ethers at

383 the oil–water interface (Camino et al., 2009; Mezdour et al., 2008), and to our best

384 knowledge none of them focused on the combined study of the three types investigated here

385 or in their competitive adsorption with bile salts. For that reason, the values of interfacial

386 tension and dilatational modulus measured after 30 min of adsorption at 20 ºC are presented

387 as a function of the bulk concentration. These are not equilibrium values, since several hours

388 are needed to attain true equilibrium: from at least 12 to 24 h for low derivatised cellulose

389 concentrations (Camino et al., 2009; Persson, Nilsson, & Sundelof, 1996). A combination of

390 slow diffusion transport of polymer to the interface and slow conformational rearrangements

391 of already adsorbed polymer is thought to cause the slow decrease in the surface tension at

392 low concentrations (Nahringbauer, 1995). Nevertheless, the adsorption process is completed

18

393 within a very short timeframe, of the order of a few seconds, at high concentrations (Mezdour

394 et al., 2007). Since this work is part of an integral study where stabilisation of oil in water

395 emulsions is involved, interfacial parameters at short timescale, 30 min or less, will provide

396 relevant information to emulsification procedures.

397 As done for the experiments in the aqueous phase, the effect of the molecular weight is first

398 considered on the interfacial activity of cellulose ethers. The interfacial behaviour of MC

399 A4C and MC A4M is compared in Figure 6a. Both types of MC lower the interfacial tension

400 to a similar extent after 30 min of adsorption, reaching a saturation value of approximately 16

401 mN/m, which is in agreement with values reported for METHOCEL™ A4M at oil–water

402 interfaces (Floury, Desrumaux, Axelos, & Legrand, 2003; Gaonkar, 1991). This is

403 presumably due to the similar hydrophobicity of A4C and A4M since the content of methyl

404 groups is the same in both kinds of MC (Table 1). Previous work showed similar interfacial

405 tension for METHOCEL™ HPMC samples of different viscosities, suggesting an interfacial

406 activity independent of the molecular weight (Gaonkar, 1991). However, the adsorption

407 dynamics should depend on the molecular weight, since the diffusion to the interface is

408 slower for larger molecules (Floury et al., 2003). Indeed, initial adsorption rates at low MC

409 concentrations (10^{-5}-10^{-3} wt%) seem to be slightly slower for the higher molecular weight

410 A4M than for the lower molecular weight A4C (results not shown). Then, the complex

411 dilatational modulus is reported at a representative frequency of 0.1 Hz (Figure 6a), since a

412 predominantly elastic response, *i.e. E' > E''*, was obtained at all frequencies and

413 concentrations tested, as reported for some cellulose derivatives at the air–water interface

414 (Perez, Sanchez, Patino, & Pilosof, 2006). Furthermore, the loss tangent that represents the

415 relationship between the viscous and elastic component of the interfacial dilatational modulus

416 (*Tanδ = E''/E'*) appears frequency independent at high concentrations, Tanδ ~ 0.2, and

417 ranging from 0.2 to 0.4 at low concentrations (data not shown). A molecular weight-

418   dependence would be also expected for the viscoelasticity of MC interfacial layers (Floury et

419   al., 2003). At a certain interfacial concentration, the resistance to dilatation/compression

420   deformation depends on the interactions of the molecules adsorbed at the interface and

421   adsorption rate of molecules present in the surrounding aqueous phase, which in turn will

422   depend on the molecular size, among other properties. Interestingly, both types of MC

423   display the same dilatational response (Figure 6a). Similar viscoelasticity between HPMC

424   samples of different molecular weight but similar degree of methyl substitution was also

425   found by Pérez and co-workers (Perez et al., 2006). Hence, it seems that, in the studied

426   molecular weight range, the interactions between hydrophobic segments actually in contact

427   with the interface account for the measured dilatational modulus. It is then reasonable to

428   think that the similar dilatational response found for MCs might be due to similar proportion

429   of interacting methyl substituents adsorbed at the interface. The presence of two maxima in

430   the dilatational modulus (Figure 6a) suggests at least two changes in interfacial conformation

431   upon increasing the concentration. The first maximum is located at a bulk concentration

432   corresponding to the initial decrease in interfacial tension, just before the abrupt drop. The

433   formation of trains, loops and tails is likely to occur (Wollenweber, Makievski, Miller, &

434   Daniels, 2000), having rearrangements on the interfacial layer with adsorbed molecules going

435   from a more expanded configuration to a more condensed one (Li, Xu, Xin, Cao, & Wu,

436   2008; Perez et al., 2006). Then, the second maximum is found at a higher bulk concentration

437   corresponding to the plateau in the interfacial tension, where a saturated interface has been

438   reached. It seems that at higher interfacial coverage, MC molecules continue rearranging,

439   forming a more condensed interfacial layer or even multilayers, as reported for HPMC at air–

440   water and oil–water interfaces (Perez et al., 2006; Wollenweber et al., 2000).
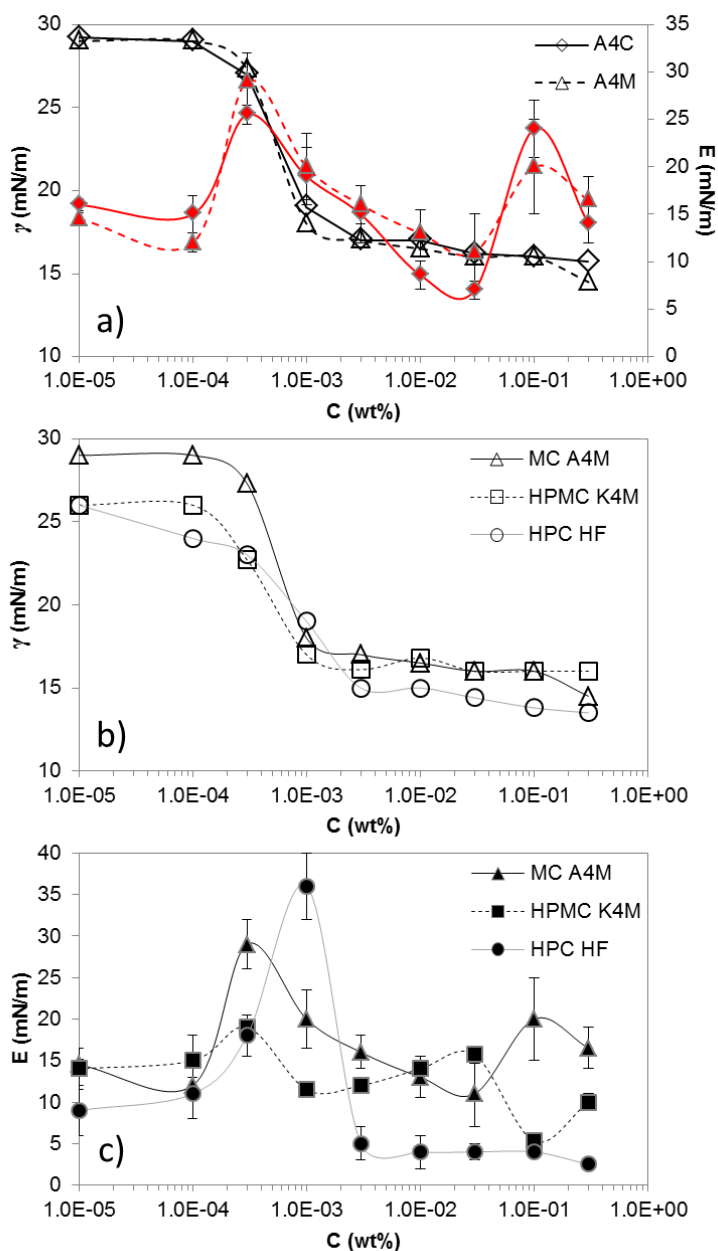
441

Figure 6: Interfacial tension (open symbols) and dilatational modulus (closed symbols) (f = 0.1 Hz) of a) MC solutions (low molecular weight, A4C; high molecular weight, A4M), b) and c) cellulose ethers solutions (MC A4M; HPMC K4M; HPC HF) at the olive oil–water interface as a function of the bulk concentration (T = 20 ºC, 30 min of adsorption). Error bars are within the size of the symbols for the interfacial tension values.

447

448   Next, the effect of the type and number of substituents on the interfacial activity is evaluated

449   for the set of cellulose derivatives within the similar range of viscosity (Figure 6b,c). In this

450   case, appreciable differences can be observed in the interfacial behaviour. Interfacial activity

451   of MC and HPC are first compared. HPC lowers the interfacial tension to a larger extent than

452   MC within practically the whole range of concentration, after 30 min of adsorption (Figure

453   6b). Also, the initial decrease in the interfacial tension at lower concentrations is more

454   gradual for HPC. The larger number and size of hydroxypropyl groups in HPC would

455   eventually occupy larger interfacial area than methyl groups in MC, which is related with

456   larger decrease in the interfacial tension. Previous studies showed lower surface tension for

457   HPC, while MC and HPMC displayed similar but higher surface tension (Arboleya & Wilde,

458   2005; Mezdour et al., 2007; Persson et al., 1996). Hence, an analogous behaviour is found at

459   both air–water and oil–water interfaces. However, hydroxypropyl groups present a more

460   polar character than methyl groups, which is reflected in slower adsorption rates of HPC at

461   low bulk concentrations: 10^{-5}-10^{-2} wt% (data not shown). On the other hand, the breakpoint

462   of the interfacial tension between the low and high polymer concentration regimes, denoted

463   as critical aggregation concentration (CAC), which is characteristic for a given polymer, and

464   is related with the critical micelle concentration of low molecular weight surfactants, seems

465   to be higher for HPC. However, it has to be taken into account that these are not equilibrium

466   values. When the adsorption of a 10^{-3} wt% HPC solution was measured after 1 h, the

467   interfacial tension reached a value of 16.5 mN/m. Hence, this concentration is the CAC after

468   1 h of adsorption, for both MC and HPC. This agrees with the similar CAC values found for

469   HPC and different HPMCs, suggesting that the molecular weight and the type and degree of

470   substitution have a low influence on CAC (Persson et al., 1996; Wollenweber et al., 2000).

471   Regarding the dilatational behaviour (Figure 6c), some differences can be seen in the location

472   of the first maximum in the dilatational modulus at lower interfacial coverage and the missing

473 second maximum of HPC at higher interfacial coverage. The first maximum appears at higher

474 bulk concentration for HPC than for MC, corresponding also to a larger decrease in the

475 interfacial tension of HPC, as compared to the interfacial tension of MC. It is likely that HPC

476 chains lay in a more expanded structure than MC at the interface, at lower concentrations,

477 due to the more "uniform" distribution of substituents. This would also contribute to the

478 larger decrease in the interfacial tension at lower interfacial coverage for HPC. Then, the

479 polymer chains would rearrange, as in the case of MC, into a brush-like conformation upon

480 increasing the interfacial coverage (Mezdour et al., 2008). However, HPC does not show the

481 second maximum in the dilatational modulus as MC, suggesting that it does not change the

482 interfacial configuration within the regime of high concentration. HPC interfacial structure

483 might become more condensed instead, upon further increasing the bulk concentration, as

484 seen by the continuous decrease in interfacial tension at higher interfacial coverage.

485 Differently for MC, the formation of multilayers might be possible, as reflected by the second

486 maximum (Figure 6c).

487 Finally, HPMC shows an interfacial behaviour which is in between of those of MC and HPC.

488 Within the regime of low bulk concentration, the adsorption isotherm of HPMC is similar in

489 shape to that of MC, although approaching interfacial tension values attained by HPC (Figure

490 6b). Adsorption dynamics of HPMC is slightly slower than for MC but faster than for HPC,

491 corroborating that at a certain viscosity, the more hydrophobic methyl groups in the whole

492 molecule act as a driving force for the diffusion (Perez, Sanchez, Pilosof, & Patino, 2008). In

493 addition, the first maximum in the dilatational modulus is located at the same concentration

494 as for MC, although shows lower values (Figure 6c). It seems that HPMC changes the

495 interfacial conformation in a similar way as MC, suggested by the shape in the adsorption

496 isotherm and the location of the dilatational modulus maximum, however the presence of

497 hydroxypropyl groups occupying larger interfacial area than methyl groups might explain the

498 larger decrease in the interfacial tension as compared to MC. The saturation of the interfacial

499 layer starts at the same bulk concentration of 10^{-3} wt% for MC and HPMC, in agreement with

500 literature values at air–water interface (Arboleya & Wilde, 2005), and reaching similar values

501 of the interfacial tension within the regime of high interfacial coverage (Figure 6b).

502 Nevertheless, the second maximum in the dilatational modulus appears now at lower

503 concentration for HPMC than for MC (Figure 6c). This suggests again a similar conformation

504 to that acquired for MC upon increasing the concentration, such as multilayer formation,

505 however now being attained at slightly lower interfacial coverage for HPMC. Hence, despite

506 HPMC also forms similar bundles as MC in solution, the lower degree of substitution for

507 methyl groups and the presence of hydroxypropyl groups clearly give rise to differences in

508 the interfacial behaviour.

509 There is some evidence from these results that the interfacial properties of macromolecules

510 like cellulose ethers at the oil–water interface depend on the length and distribution of trains,

511 loops and tails, analogous to the behaviour at the air–water interface (Perez et al., 2006).

512

513 *3.4. Competitive adsorption of cellulose ethers and bile salt at the oil–water interface*

514 Finally, for the competitive adsorption experiments of cellulose ethers in the presence of the

515 bile salt, we have chosen a fixed bulk concentration of cellulose derivatives of 10^{-3} wt%.

516 Such a concentration provides an almost saturated interface, given by the value of the

517 interfacial tension close to the plateau in the adsorption isotherm (Figure 6b), and a

518 dilatational modulus close to the first maximum (Figure 6c), when a brush-like conformation

519 has been reached. In this section, the interfacial tension and dilatational modulus of mixtures

520 of cellulose ethers and bile salt after 30 min of adsorption at the oil–water interface are

521 displayed as a function of the bile salt concentration (Figure 7). Results are discussed

522 comparing with the interfacial behaviour of the bile salt alone, referred as control in Figure 7.
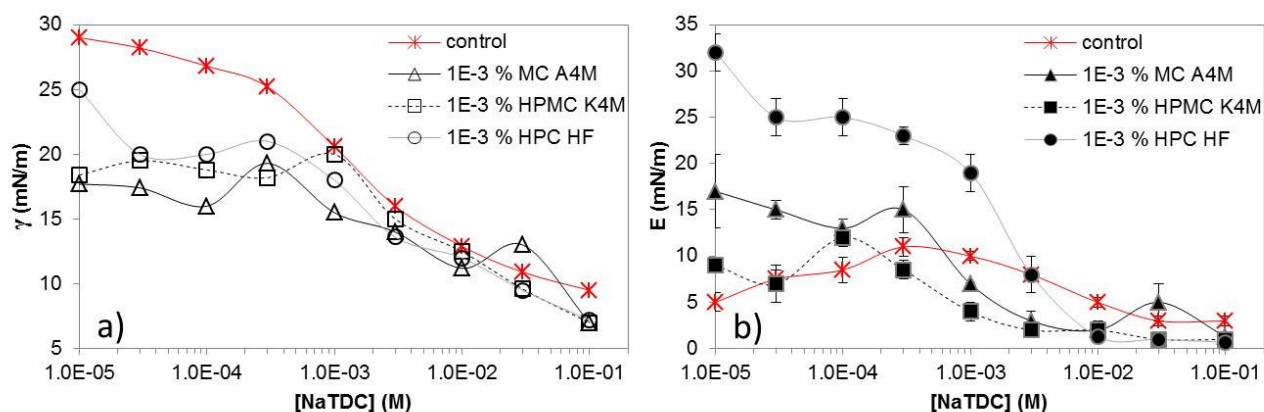
523

524

Figure 7: a) Interfacial tension (error bars are within the size of the symbols) and b)

dilatational modulus (f = 0.1 Hz) of mixtures of 10^{-3} wt% cellulose ethers (MC A4M; HPMC

K4M; HPC HF) and bile salt (NaTDC) solutions at the olive oil–water interface as a function

of the bile salt bulk concentration (T = 20 ºC, 30 min of adsorption).

529

At the lowest bile salt concentration, mixtures attain interfacial tension (Figure 7a) and

dilatational modulus (Figure 7b) values similar to those of cellulose ethers in the absence of

the bile salt (Figure 6b,c). Also, the adsorption rate is similar to that for cellulose derivatives

alone (data not shown). This means that the process of adsorption is being controlled by the

cellulose derivatives and that the adsorbed layer is mainly composed of cellulose ethers even

after 30 min of adsorption. The only exception is found for the mixture of HPC and bile salt,

with higher interfacial tension than for HPC alone, although the dynamics of adsorption and

dilatational modulus agree with that for HPC alone. When increasing the bile salt

concentration in the mixtures, the rates of adsorption remain similar to those for cellulose

ethers alone, however the dynamic and final interfacial tension start to be affected when

approaching the concentration of bile salt of 10^{-3} M. It can be seen that upon further

increasing the concentration of bile salt in the mixtures, adsorption isotherms (Figure 7a) and

dilatational moduli (Figure 7b) of mixed systems approach those of pure bile salt, *i.e.* control.

543   In addition, the adsorption dynamics are similar to those of bile salt alone at the different

544   concentrations, *i.e.* fast initial adsorption rates attaining a steady interfacial tension in less

545   than 2 min, as compared with cellulose ethers which attain a steady interfacial tension in at

546   least 10 min at the concentration of 10^{-3} wt% (results not shown). This suggests that the

547   adsorption is being controlled by the bile salt. This physiological surfactant is very efficient

548   at occupying the oil–water interface, competing with other surface active molecules or even

549   displacing those already adsorbed at the interface, due to a combination of fast adsorption and

550   planar shape (Maldonado-Valderrama et al., 2011; Torcello-Gómez, Jódar-Reyes,

551   Maldonado-Valderrama, & Martin-Rodriguez, 2012). The order in which the molecules

552   arrive at the interface will influence the final interfacial composition (Damodaran &

553   Rammovsky, 2003; Ridout, Mackie, & Wilde, 2004). However, the composition of the

554   interface may change with time. Molecules that are initially at the interface may be displaced

555   by the molecules in the bulk that have a greater affinity for the interface (Baeza, Sanchez,

556   Pilosof, & Patino, 2005). Here, it seems that although bile salts are controlling the rates of

557   adsorption from the initial moments, cellulose ethers are also contributing to the decrease of

558   the interfacial tension since a lower value is obtained, as compared to the behaviour of bile

559   salt alone, throughout the whole process of adsorption (results not shown). Interestingly, even

560   at the highest bile salt concentration, the mixtures lower the interfacial tension to a larger

561   extent than pure bile salt, and also show lower dilatational response, meaning a less elastic

562   and less structured interface. This indicates coexistence of both cellulose and bile salt at the

563   oil–water interface. It might be possible that the presence of interfacial derivatised cellulose–

564   bile salt complexes account for this further decrease in the interfacial tension, with a

565   synergistic effect. Similar properties were found in our previous study on competitive

566   adsorption between triblock copolymers and this bile salt at the olive oil–water interface

567   (Torcello-Gómez et al., 2013). We have proven that all types of cellulose ethers studied in the

568 current work are able to compete for a hydrophobic interface with the bile salt. This is a very

569 important result from the viewpoint of controlling lipid digestibility, since cellulose

570 derivatives may compete with the bile salts for the oil–water interface of emulsified lipids

571 within the duodenum. The ability of derivatised cellulose to adsorb to an oil–water interface

572 in the presence of bile salts might be partially due to the sequestration of bile salts in the bulk

573 through the binding to cellulose ethers, as indicated by micro-DSC experiments of mixed

574 systems in the aqueous phase.

575

576 CONCLUSIONS

577 We have proven that the presence of bile salt affects the thermal transition undergone by

578 cellulose ethers upon heating and cooling. This inhibition by the bile salt depends on the

579 mechanism of thermogelation, which in turn will be determined by the type and number of

580 substituents in cellulose ethers. The effect is increased by increasing the ratio bile

581 salt/cellulose ether. Thermogelation of MC seems to be less susceptible to the presence of

582 bile salt than HPMC and HPC, due to the hidden methyl groups in the bundles, which allow

583 the intermolecular association to take place after exposing them upon heating. This inhibition

584 in thermal transition of cellulose derivatives reflects that interactions between bile salt and

585 cellulose ethers are taking place in the aqueous phase, supporting the mechanism of binding

586 of bile salt to dietary fibre. They might also have implications in the control of lipid digestion

587 in the sense that may have an impact on the surface of lipid droplets in emulsions, since

588 cellulose ethers compete with the bile salt for the oil–water interface even at high bile salt

589 concentrations relevant to physiological conditions within the duodenum.

590 These findings would allow the development of both functional foods and pharmacological

591 matrices with tailored biological activities, such as control of satiety and targeted release of

592 bioactive components to specific locations in the gastrointestinal tract.

593

598

599   REFERENCES

600   Anderson, J. W., & Siesel, A. E. (1990). Hypocholesterolemic Effects of Oat Products. In I.

601   Furda, & C. J. Brine (Eds.), *New Developments in Dietary Fiber: Physiological, and*

602   *Analytical Aspects* (Vol. 270, pp. 17-36). New York: Plenum Press.

603   Arboleya, J. C., & Wilde, P. J. (2005). Competitive adsorption of proteins with

604   methylcellulose and hydroxypropyl methylcellulose. *Food Hydrocolloids, 19*(3), 485-491.

605   Baeza, R., Sanchez, C. C., Pilosof, A. M. R., & Patino, J. M. R. (2005). Interactions of

606   polysaccharides with beta-lactoglobulin adsorbed films at the air-water interface. *Food*

607   *Hydrocolloids, 19*(2), 239-248.

608   Beysseriat, M., Decker, E. A., & McClements, D. J. (2006). Preliminary study of the

609   influence of dietary fiber on the properties of oil-in-water emulsions passing through an in

610   vitro human digestion model. *Food Hydrocolloids, 20*(6), 800-809.

611   Camino, N. A., Perez, O. E., Sanchez, C. C., Patino, J. M. R., & Pilosof, A. M. R. (2009).

612   Hydroxypropylmethylcellulose surface activity at equilibrium and adsorption dynamics at the

613   air-water and oil-water interfaces. *Food Hydrocolloids, 23*(8), 2359-2368.

614   Damodaran, S., & Rammovsky, L. (2003). Competitive adsorption and thermodynamic

615   incompatibility of mixing of beta-casein and gum arabic at the air-water interface. *Food*

616   *Hydrocolloids, 17*(3), 355-363.

617   Fave, G., Coste, T. C., & Armand, M. (2004). Physicochemical properties of lipids: New

618   strategies to manage fatty acid bioavailability. *Cellular and Molecular Biology, 50*(7), 815-

619   831.

620   Floury, J., Desrumaux, A., Axelos, M. A. V., & Legrand, J. (2003). Effect of high pressure

621   homogenisation on methylcellulose as food emulsifier. *Journal of Food Engineering, 58*(3),

622   227-238.

623   Gaonkar, A. G. (1991). Surface and Interfacial Activities and Emulsion Characteristics of

624   Some Food Hydrocolloids. *Food Hydrocolloids, 5*(4), 329-337.

625   Gunness, P., Flanagan, B. M., & Gidley, M. J. (2010). Molecular interactions between cereal

626   soluble dietary fibre polymers and a model bile salt deduced from C-13 NMR titration.

627   *Journal of Cereal Science, 52*(3), 444-449.

628   Haque, A., & Morris, E. R. (1993). Thermogelation of Methylcellulose .1. Molecular-

629   Structures and Processes. *Carbohydrate Polymers, 22*(3), 161-173.

630   Haque, A., Richardson, R. K., Morris, E. R., Gidley, M. J., & Caswell, D. C. (1993).

631   Thermogelation of Methylcellulose .2. Effect of Hydroxypropyl Substituents. *Carbohydrate*

632   *Polymers, 22*(3), 175-186.

633   Jenkins, D. J. A., Kendall, C. W. C., & Ransom, T. P. P. (1998). Dietary fiber, the evolution

634   of the human diet and coronary heart disease. *Nutrition Research, 18*(4), 633-652.

635   Kritchevsky, D., & Story, J. A. (1993). Influence of dietary fiber on cholesterol metabolism

636   in experimental animals. In G. A. Spiller (Ed.), *CRC Handbook of Dietary Fiber in Human*

637   *Nutrition* (pp. 163-178). Boca Raton: CRC Press.

638   Lairon, D. (1996). Dietary fibres: Effects on lipid metabolism and mechanisms of action.

639   *European Journal of Clinical Nutrition, 50*(3), 125-133.

640   Lee, J. K., Kim, S. U., & Kim, J. H. (1999). Modification of chitosan to improve its

641   hypocholesterolemic capacity. *Bioscience Biotechnology and Biochemistry, 63*(5), 833-839.

642   Li, Y. M., Xu, G. Y., Xin, X., Cao, X. R., & Wu, D. (2008). Dilational surface viscoelasticity

643   of hydroxypropyl methyl cellulose and C(n)TAB at air-water surface. *Carbohydrate*

644   *Polymers, 72*(2), 211-221.

645   Maldonado-Valderrama, J., Wilde, P., Macierzanka, A., & Mackie, A. (2011). The role of

646   bile salts in digestion. *Advances in Colloid and Interface Science, 165*(1), 36-46.

647   Mezdour, S., Cuvelier, G., Cash, M. J., & Michon, C. (2007). Surface rheological properties

648   of hydroxypropyl cellulose at air-water interface. *Food Hydrocolloids, 21*(5-6), 776-781.

649   Mezdour, S., Lepine, A., Erazo-Majewicz, P., Ducept, F., & Michon, C. (2008). Oil/water

650   surface rheological properties of hydroxypropyl cellulose (HPC) alone and mixed with

651   lecithin: Contribution to emulsion stability. *Colloids and Surfaces a-Physicochemical and*

652   *Engineering Aspects, 331*(1-2), 76-83.

653   Nahringbauer, I. (1995). Dynamic surface tension of aqueous polymer solutions .1.

654   Ethyl(hydroxyethyl)cellulose (BERMOCOLL cst-103). *Journal of Colloid and Interface*

655   *Science, 176*(2), 318-328.

656   Perez, O. E., Sanchez, C. C., Patino, J. M. R., & Pilosof, A. M. R. (2006). Thermodynamic

657   and dynamic characteristics of hydroxypropylmethylcellulose adsorbed films at the air-water

658   interface. *Biomacromolecules, 7*(1), 388-393.

659   Perez, O. E., Sanchez, C. C., Pilosof, A. M. R., & Patino, J. M. R. (2008). Dynamics of

660   adsorption of hydroxypropyl methylcellulose at the air-water interface. *Food Hydrocolloids,*

661   *22*(3), 387-402.

662   Persson, B., Nilsson, S., & Sundelof, L. O. (1996). On the characterization principles of some

663   technically important water-soluble nonionic cellulose derivatives .2. Surface tension and

664   interaction with a surfactant. *Carbohydrate Polymers, 29*(2), 119-127.

665   Reis, P., Holmberg, K., Watzke, H., Leser, M. E., & Miller, R. (2009). Lipases at interfaces:

666   A review. *Advances in Colloid and Interface Science, 147-48*, 237-250.

667   Ridout, M. J., Mackie, A. R., & Wilde, P. J. (2004). Rheology of mixed beta-casein/beta-

668   lactoglobulin films at the air-water interface. *Journal of Agricultural and Food Chemistry,*

669   *52*(12), 3930-3937.

670   Sarkar, N. (1979). Thermal Gelation Properties of Methyl and Hydroxypropyl

671   Methylcellulose. *Journal of Applied Polymer Science, 24*(4), 1073-1087.

672   Story, J. A., Furumoto, E. J., & Buhman, K. K. (1997). Dietary fiber and bile acid

673   metabolism - an update. In D. Kritchevsky, & C. Bonfield (Eds.), *Dietary Fiber in Health*

674   *and Disease* (Vol. 427, pp. 259-266). New York: Plenum Press.

675   Sullo, A., Wang, Y. H., Koschella, A., Heinze, T., & Foster, T. J. (2013). Self-association of

676   novel mixed 3-mono-O-alkyl cellulose: Effect of the hydrophobic moieties ratio.

677   *Carbohydrate Polymers, 93*(2), 574-581.

678   Sun, S. M., Foster, T. J., MacNaughtan, W., Mitchell, J. R., Fenn, D., Koschella, A., &

679   Heinze, T. (2009). Self-Association of Cellulose Ethers with Random and Regioselective

680   Distribution of Substitution. *Journal of Polymer Science Part B-Polymer Physics, 47*(18),

681   1743-1752.

682   Thongngam, M., & McClements, D. J. (2005). Isothermal titration calorimetry study of the

683   interactions between chitosan and a bile salt (sodium taurocholate). *Food Hydrocolloids,*

684   *19*(5), 813-819.

685   Tokle, T., Lesmes, U., Decker, E. A., & McClements, D. J. (2012). Impact of dietary fiber

686   coatings on behavior of protein-stabilized lipid droplets under simulated gastrointestinal

687   conditions. *Food & Function, 3*(1), 58-66.

688   Torcello-Gómez, A., Jódar-Reyes, A. B., Maldonado-Valderrama, J., & Martin-Rodriguez,

689   A. (2012). Effect of emulsifier type against the action of bile salts at oil-water interfaces.

690   *Food Research International, 48*(1), 140-147.

691   Torcello-Gómez, A., Maldonado-Valderrama, J., Jódar-Reyes, A. B., & Foster, T. J. (2013).

692   Interactions between Pluronics (F127 and F68) and Bile Salts (NaTDC) in the Aqueous Phase

693   and the Interface of Oil-in-Water Emulsions. *Langmuir, 29*(8), 2520-2529.

694   Vahouny, G. V., Satchithanandam, S., Chen, I., Tepper, S. A., Kritchevsky, D., Lightfoot, F.

695   G., & Cassidy, M. M. (1988). Dietary Fiber and Intestinal Adaptation - Effects on Lipid

696   Absorption and Lymphatic Transport in the Rat. *American Journal of Clinical Nutrition,*

697   *47*(2), 201-206.

698   Wollenweber, C., Makievski, A. V., Miller, R., & Daniels, R. (2000). Adsorption of

699   hydroxypropyl methylcellulose at the liquid/liquid interface and the effect on emulsion

700   stability. *Colloids and Surfaces a-Physicochemical and Engineering Aspects, 172*(1-3), 91-

701   101.

702   Yokoyama, W., Anderson, W. H. K., Albers, D. R., Hong, Y. J., Langhorst, M. L., Hung, S.

703   C., Lin, J. T., & Young, S. A. (2011). Dietary Hydroxypropyl Methylcellulose Increases

704   Excretion of Saturated and Trans Fats by Hamsters Fed Fast Food Diets. *Journal of*

705   *Agricultural and Food Chemistry, 59*(20), 11249-11254.

706   Zarras, P., & Vogl, O. (1999). Polycationic salts as bile acid sequestering agents. *Progress in*

707   *Polymer Science, 24*(4), 485-516.

708

709

710

711

712

713

714

715

716 FIGURE CAPTIONS:

717 **Figure 1:** Micro-DSC traces on heating and on cooling of a) 1 wt% MC solutions: low

718 molecular weight, A4C; high molecular weight, A4M; b) 1 wt% cellulose ether solutions; left

719 axis: MC A4M; HPC HF; right axis: HPMC K4M. Transition enthalpy values on heating and

720 on cooling are given in $J/g_{polymer}$.

721

722 **Figure 2:** Schematic representation of the hypothetical structures and processes involved in

723 the thermal transition of cellulose ethers, HPC and MC, in the absence and presence of the

724 bile salt. Faint lines in cellulose ethers denote unsubstituted or sparingly substituted chain

725 segments; bold lines denote regions of dense substitution. See text for detailed description.

726

727 **Figure 3:** Micro-DSC traces on heating and on cooling of 0.3 and 1 wt% cellulose ether

728 solutions: a) MC A4M; b) HPC HF. Transition enthalpy values on heating and on cooling are

729 given in $J/g_{polymer}$.

730

731 **Figure 4:** Micro-DSC traces on heating and on cooling of mixtures of 1 wt% cellulose ether

732 solutions and bile salt at several concentrations: a) MC A4M; b) HPMC K4M; c) HPC HF.

733

734 **Figure 5:** Decrease in transition enthalpy of cellulose ethers caused by the presence of the

735 bile salt: a) effect of the type and number of substituents; b) effect of bulk concentration.

736

737 **Figure 6:** Interfacial tension (open symbols) and dilatational modulus (closed symbols) (f =

738 0.1 Hz) of a) MC solutions (low molecular weight, A4C; high molecular weight, A4M), b)

739 and c) cellulose ethers solutions (MC A4M; HPMC K4M; HPC HF) at the olive oil–water

740 interface as a function of the bulk concentration (T = 20 ºC, 30 min of adsorption). Error bars

741 are within the size of the symbols for the interfacial tension values.

742

743 **Figure 7:** a) Interfacial tension (error bars are within the size of the symbols) and b)

744 dilatational modulus (f = 0.1 Hz) of mixtures of 10^{-3} wt% cellulose ethers (MC A4M; HPMC

745 K4M; HPC HF) and bile salt (NaTDC) solutions at the olive oil–water interface as a function

746 of the bile salt bulk concentration (T = 20 ºC, 30 min of adsorption).

747